Diffusion-induced instability in chemically reacting systems: Steady-state multiplicity, oscillation, and chaos

István Lengyel[a] and Irving R. Epstein
Department of Chemistry and Center for Complex Systems, Brandeis University, Waltham, Massachusetts 02254-9110

The dynamical behavior of two coupled cells or reactors is described. The cells are coupled by diffusion, e.g., through a semipermeable membrane, and the chemical reactions and initial or feed concentrations of all species are the same in the two cells. Each cell has only a single stable steady state in the absence of coupling, and the coupled system may exhibit multiple steady states, periodic oscillation, or chaos. The attractors of the coupled system may be either homogeneous (the two cells have equal concentrations) or inhomogeneous. Three two-variable kinetic models are examined: the Brusselator, a model of the chlorine dioxide–iodine–malonic acid reaction, and the Degn–Harrison model. The dynamical behavior of the coupled system is determined by the nonlinearities in the uncoupled subsystems and by two ratios, that of the diffusion constants of the two species and that of the area of the membrane to the product of the membrane thickness and the volume of a cell.

I. INTRODUCTION

Many dynamical problems of physical and biological interest involve systems that consist of two or more coupled chemically reacting subsystems. The coupling of two reactors or cells may be accomplished in a variety of ways. For example, mass exchange,[1] electrical coupling,[2] and chemical reactions[3] have all been employed in studies of coupled chemical oscillators. The mass exchange may be diffusive, in which the diffusion coefficients of the reacting species can differ, or it may be convective, so that all "diffusion coefficients" are the same. Diffusion may be Fickian or concentration dependent. One may envision many combinations of uncoupled states in the individual reactors. In the limit of zero coupling, each subsystem may show steady state or oscillatory behavior, and, depending upon the parameters (input concentrations, rate constants), the two reactors may possess the same or different attractors. In this paper we treat the case of two reactors that have the same unique stable steady state and that are coupled by Fickian diffusion.

One normally thinks of diffusion as acting to equalize concentration differences in space. However, as Turing showed[4] nearly 4 decades ago in a remarkable paper entitled "The Chemical Basis of Morphogenesis," diffusion can have the opposite effect. When diffusion is coupled to suitable chemical reactions, it can destabilize a stable homogeneous steady state, generating stable, time-independent concentration gradients. Turing's work has become the basis for an important approach to modeling spatial structure in biological systems, from patterns on animal coats to cluster formation in bacterial cultures. The literature on the subject is extensive; we mention here the books by Meinhardt[5] and Murray.[6] Most work has been done for the case of distributed spatial one-dimensional systems, but as Turing showed, diffusion-induced instability can also occur when two homogeneous cells are coupled. Prigogine and Lefever[7] demonstrated the existence of diffusion-induced instability in a two-cell configuration using the Brusselator model for the kinetics. Later, Tyson and Kauffman[8] reinvestigated the problem, performing thorough analytical studies of that model, primarily for the case of two coupled oscillatory Brusselators. Schreiber et al.[9] carried out numerical studies of the same system and found stabilization of homogeneous oscillations, various types of homogeneous and inhomogeneous oscillations, phase locking, and chaos. Ortoleva and Ross[10] described a mechanism for asymmetric cell differentiation based on diffusion-induced instability with a Brusselator-like cubic autocatalytic scheme for the kinetics.

Here we treat a system of two reactors in which the same chemical reactions occur with the same parameters. The reactors are coupled through a permeable wall through which all species can diffuse. The parameters (rate constants, input concentrations) are such that in the absence of the coupling, each reaction has the same unique attractor, a stable steady state. We first examine a general two-variable kinetic model and obtain analytically the necessary and sufficient conditions for this stable homogeneous steady state to lose stability as a result of the coupling. We then analyze numerically several models and show that diffusion-induced instability can lead to multiple stable steady states, oscillatory states, and, in the most complicated example, chaos.

II. DESCRIPTION OF THE PROBLEM

Consider the experimental configuration shown in Fig. 1, in which two well-stirred reactors are connected by a common wall composed of a membrane through which chemicals can diffuse by Fickian diffusion. The width of the wall is negligible compared to the size of the system, so

---

[a] Permanent address: Institute of Physical Chemistry, Kossuth Lajos University, Debrecen, H-4010 Hungary.
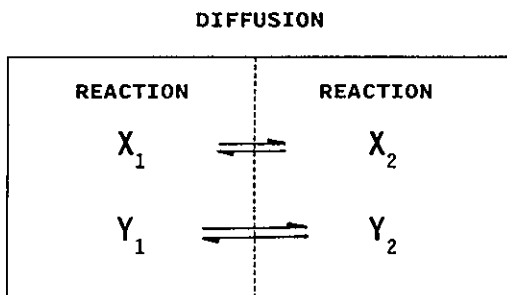
DIFFUSION

FIG. 1. Schematic diagram of a coupled reactor system.

that no species accumulate in the membrane, and the time spent crossing the membrane may be neglected.[11] If this approximation does not hold, the membrane must be considered as an open spatial reactor in which diffusion can occur not only perpendicular to the surface but parallel as well. In the latter case, which we do not treat here, the system is much more complicated, and can give rise to wave behavior and pattern formation in the membrane.[12] The coupling between the reactors depends on the volumes (V_i) of the individual reactors, the surface area (A), and the thickness (l) of the membrane. We define the parameter c_i, $i = 1,2$, which measures the strength of this coupling,

$$c_i = A/V_i l. \tag{1}$$

III. STABILITY ANALYSIS

Consider a two-variable homogeneous reaction described by the differential equation system

$$\dot{x} = f(x,y), \tag{2}$$

$$\dot{y} = g(x,y).$$

For the parameter set of interest the system has a single stable steady state (x_{ss}, y_{ss}). If we couple the system (2) with an identical system in a configuration like that shown in Fig. 1, the resulting four-variable coupled system is described by

$$\dot{x}_1 = f(x_1,y_1) + D_x c_1 (x_2 - x_1),$$

$$\dot{y}_1 = g(x_1,y_1) + D_y c_1 (y_2 - y_1),$$

$$\dot{x}_2 = f(x_2,y_2) - D_x c_2 (x_2 - x_1), \tag{3}$$

$$\dot{y}_2 = g(x_2,y_2) - D_y c_2 (y_2 - y_1),$$

where D_x and D_y are the diffusion coefficients of the respective species.

Clearly, one solution of the system (3) is the homogeneous steady state (HSS) in which $x_1 = x_2 = x_{ss}$, $y_1 = y_2 = y_{ss}$. It is obvious that the homogeneous steady state is stable against homogeneous perturbations for which the perturbation is the same in both reactors. However, the HSS is not necessarily stable to inhomogeneous perturbations in which the magnitude and/or sign of the perturbation differs in the two reactors. We seek, using simple linear stability analysis, conditions for the coupling strengths

c_i and diffusion coefficients D_j such that an infinitesimal inhomogeneous perturbation of the HSS grows in time. To facilitate the analysis, we introduce sum and difference variables:

$$s = x_1 + x_2, \quad \Sigma = y_1 + y_2,$$
$$d = x_1 - x_2, \quad \Delta = y_1 - y_2. \tag{4}$$

The transformed differential equation system is then:

$$\dot{s} = f\left(\frac{s+d}{2}, \frac{\Sigma+\Delta}{2}\right) + f\left(\frac{s-d}{2}, \frac{\Sigma-\Delta}{2}\right)$$
$$\quad - D_x(c_1 - c_2)d,$$

$$\dot{\Sigma} = g\left(\frac{s+d}{2}, \frac{\Sigma+\Delta}{2}\right) + g\left(\frac{s-d}{2}, \frac{\Sigma-\Delta}{2}\right)$$
$$\quad - D_y(c_1 - c_2)\Delta, \tag{5}$$

$$\dot{d} = f\left(\frac{s+d}{2}, \frac{\Sigma+\Delta}{2}\right) - f\left(\frac{s-d}{2}, \frac{\Sigma-\Delta}{2}\right)$$
$$\quad - D_x(c_1 + c_2)d,$$

$$\dot{\Delta} = g\left(\frac{s+d}{2}, \frac{\Sigma+\Delta}{2}\right) - g\left(\frac{s-d}{2}, \frac{\Sigma-\Delta}{2}\right)$$
$$\quad - D_y(c_1 + c_2)\Delta.$$

One solution of the system (5) is the HSS, which is given in terms of the new variables by

$$s_{ss} = 2x_{ss}, \quad d_{ss} = 0,$$
$$\Sigma_{ss} = 2y_{ss}, \quad \Delta_{ss} = 0. \tag{6}$$

On linearizing the system around this steady state, we find that the Jacobian has a special form:

$$\begin{pmatrix} a_{11} & a_{12} & D_x(c_2 - c_1) & 0 \\ a_{21} & a_{22} & 0 & D_y(c_2 - c_1) \\ 0 & 0 & a_{11} - D_x(c_1 + c_2) & a_{12} \\ 0 & 0 & a_{21} & a_{22} - D_y(c_1 + c_2) \end{pmatrix}, \tag{7}$$

where a_{ij} is the Jacobian element of the uncoupled subsystem (2) at the HSS solution. The Jacobian (7) has four eigenvalues, but because of its special structure, we need investigate only the two that belong to the bottom right 2×2 matrix, because the upper left 2×2 matrix gives the uncoupled HSS eigenvalues. These do not change with either the diffusion coefficients or with c, and they have negative real parts, since we have assumed that the uncoupled HSS is stable.

Let A be the bottom right 2×2 matrix:

$$A = \begin{pmatrix} a_{11} - D_x c & a_{12} \\ a_{21} & a_{22} - D_y c \end{pmatrix}, \quad \text{where } c = c_1 + c_2. \tag{8}$$

When the real part of one of the eigenvalues of A changes sign, the HSS becomes unstable and diffusion-induced instability appears. The stability of the uncoupled ($c = 0$) HSS implies that

$$a_{11} + a_{22} < 0, \tag{9a}$$

$$a_{11}a_{22} - a_{12}a_{21} > 0. \tag{9b}$$

When $c \neq 0$, a steady state of the coupled system is stable if

$$a_{11} - D_x c + a_{22} - D_y c < 0, \tag{10a}$$

$$(a_{11} - D_x c)(a_{22} - D_y c) - a_{12}a_{21} > 0. \tag{10b}$$

If either inequality (10a) or (10b) is violated, the homogeneous steady state in the coupled system will be unstable. Because $D_x, D_y, c > 0$, (10a) always holds so long as (9a) is true. Diffusion-induced instability thus appears if condition (10b) is violated, i.e., if

$$H(c) = D_x D_y c^2 - (D_x a_{11} + D_y a_{22})c$$
$$+ (a_{11}a_{22} - a_{12}a_{21}) < 0. \tag{11}$$

The graph of $H(c)$ is a parabola that opens upward. A necessary and sufficient condition for diffusion-induced instability is that $H(c_{\min}) < 0$, where the minimum of $H(c)$ occurs at

$$c_{\min} = \frac{1}{2}\left(\frac{a_{11}}{D_y} + \frac{a_{22}}{D_x}\right). \tag{12}$$

When $H(c_{\min}) < 0$, $H(c)$ has two zeros, and diffusion-induced instability exists between these values of c. Outside this range the homogeneous steady state is stable. Substituting (12) into (11) we obtain

$$(a_{11}n + a_{22}) > 2\sqrt{n(a_{11}a_{22} - a_{12}a_{21})}$$
$$> 0, \quad \text{where } n = D_y/D_x. \tag{13}$$

Comparing the first term of Eq. (13) with Eq. (9a), we see that a_{11} and a_{22} must be of opposite sign. For specificity, suppose that a_{11} is positive. Then diffusion-induced instability can occur only if $n > 1$. In the standard terminology used in the investigation of Turing instabilities, the species (here x) that gives a positive diagonal element in the Jacobian is called the activator, while the one with a negative diagonal element (y) is the inhibitor. The activator can be an autocatalytic species or a reactant that inhibits its own consumption. The inhibitor consumes the autocatalyst or increases the concentration of inhibitory species. For the homogeneous steady state to be unstable it is necessary that the diffusion coefficient of the inhibitor be greater than that of the activator. An increase in the ratio n shifts $H(c)$ downward and broadens the range of c in which the HSS is unstable. There is a minimum value of n, at which $H(c_{\min}) = 0$. At lower n, $H(c)$ has no real roots and the homogeneous steady state is stable for all values of c.

The analysis and the results obtained here are very similar to the treatment of the continuous reaction-diffusion problem in one spatial dimension that describes Turing instabilities.[6,13,14] Here, however, the relevant stability parameter is c, which is related to the geometry of the reactor, while in the continuous case the relevant parameter is the wavelength of the perturbation. The critical ratio of diffusion coefficients is the same in the two cases, which is not surprising, because the phenomenon considered here is a form of Turing instability.

The above analysis allows us to find where the homogeneous steady state becomes unstable. We next ask what

TABLE I. Symbols and labels in the bifurcation diagrams.

Symbol/Label	Description
—	stable steady state in one-parameter bifurcation diagrams or pitchfork bifurcation line in two-parameter bifurcation diagrams
---	unstable steady state in one-parameter bifurcation diagrams or inhomogeneous Hopf bifurcation line in two-parameter bifurcation diagrams
– – –	homogeneous Hopf bifurcation line in two-parameter bifurcation diagrams
////	region of diffusion-induced instability in two-parameter bifurcation diagrams
××××	region of diffusion-induced oscillation in two-parameter bifurcation diagrams
□	pitchfork bifurcation point
■	Hopf bifurcation point
●●●	amplitude of stable limit cycle
○○○	amplitude of unstable limit cycle
P	pitchfork bifurcation point
IHB	Hopf bifurcation point of the inhomogeneous steady state
HHB	Hopf bifurcation point of the homogeneous steady state
LP	limit point
PD	period doubling bifurcation
BP	bifurcation point, other than period doubling or limit point, where stability of the limit cycle changes

new states arise and what their stability is. These questions cannot be answered generally, since the answers depend on the particular kinetic equations. For finding the new steady states and investigating their stability, continuation algorithms[15,16] provide convenient and powerful tools. We used the AUTO86 package[17] to calculate one- and two-parameter bifurcation diagrams. In some models stability conditions for the new steady states can be given in closed form as a function of the parameters, but in most cases results can only be obtained numerically. The AUTO86 package allows one to find steady-state points, determine their stability, detect codimension one bifurcation points, and follow limit and Hopf bifurcation points of an orbit in two parameters. However, because of their degeneracy, pitchfork bifurcation points cannot be followed in two parameters. In the following two-parameter bifurcation diagrams, lines of pitchfork bifurcations, where the HSS loses its stability in the coupled system, were calculated from linear stability analysis of Eq. (11).

We have chosen three models to illustrate the variety of behavior that can occur in the coupled system. The Brusselator[7] has been selected because of its simplicity and widespread application in nonlinear dynamics. The second model[18] describes the chlorine dioxide–iodine–malonic acid reaction and has been employed previously to model experimental Turing structures in continuous media.[19] Finally, the biologically motivated Degn–Harrison model[20,21] exhibits the most complex behavior found in these systems—chaos. In all cases we study reactors with equal volume, $c = c_1 = c_2$. In the analysis that follows, c is a dimensionless variable, rescaled according to each model. Table I shows the labels and symbols used in the bifurcation diagrams presented in the next three sections.

IV. THE BRUSSELATOR

The Brusselator kinetic scheme is one of the most popular models for the study of dissipative structures in nonlinear chemical systems.[22] The chemical reactions from which it is constructed are

$$
\begin{aligned}
A &\rightarrow X, \\
2X + Y &\rightarrow 3X, \\
B + X &\rightarrow Y + D, \\
X &\rightarrow E.
\end{aligned}
\tag{14}
$$

The resulting kinetic equations may be written in dimensionless form as

$$
\begin{aligned}
\dot{x} &= a - (b+1)x + x^2 y, \\
\dot{y} &= bx - x^2 y.
\end{aligned}
\tag{15}
$$

The steady state is $x_{ss} = a$, $y_{ss} = b/a$. This homogeneous steady state is stable if $b < 1 + a^2$, the only case that we investigate here. The case in which the uncoupled system is oscillatory has been thoroughly investigated by Schreiber et al.[9] Using Eqs. (11) and (13) we can calculate, for a given set (c, D_y, D_x), the region in the (a, b) parameter space in which diffusion-induced instability occurs. Figure 2(a) is a one-parameter bifurcation diagram of the system, showing the steady-state value of x vs the bifurcation parameter c. Where a pair of steady-state values is shown, the steady state is inhomogeneous: x_1 takes one of the indicated values, while x_2 takes the other. Because of the symmetry of the system, such states occur in complementary pairs with the values of x_1 and x_2 (and y_1 and y_2) reversed.

Both pitchfork bifurcations are supercritical, and the inhomogeneous state is stable when it appears at the bifurcation. At another kinetic parameter set (a, b) shown in Fig. 2(b) the inhomogeneous steady states lose stability through supercritical Hopf bifurcation. At this point, oscillation appears as a result of the diffusion-induced instability. Examination of the time series shows that the two reactors are 180° out of phase.

The two-parameter bifurcation diagram in Fig. 3 shows that for a given c and diffusion coefficient ratio n oscillatory behavior is found only in a small closed range of parameters a and b. That oscillation should occur is not obvious a priori, since in the absence of coupling we are outside the oscillatory parameter range. Boukalouch et al.[23] have observed similar diffusion-induced oscillation both in a model and in experiments on the chlorite–iodide reaction in coupled flow reactors, but with relatively large differences in the parameters (inflow concentrations) of the two reactors. In the case considered here, where the two reactors are under the same external constraints, no diffusion-induced oscillatory behavior can occur at the lower diffusion constant ratios n characteristic of most reactions involving small ions in aqueous solution.

V. A MODEL OF THE CHLORINE DIOXIDE–IODINE–MALONIC ACID REACTION

This reaction was recently shown[18,24] to be responsible for the closed system oscillation in the more complex

chlorite–iodide–malonic acid reaction system, in which the first experimental evidence for Turing structures was obtained.[25] The simple model[18] shown in Eqs. (17) gives quantitative agreement with the experimental range of reactant concentrations where oscillations appear and was

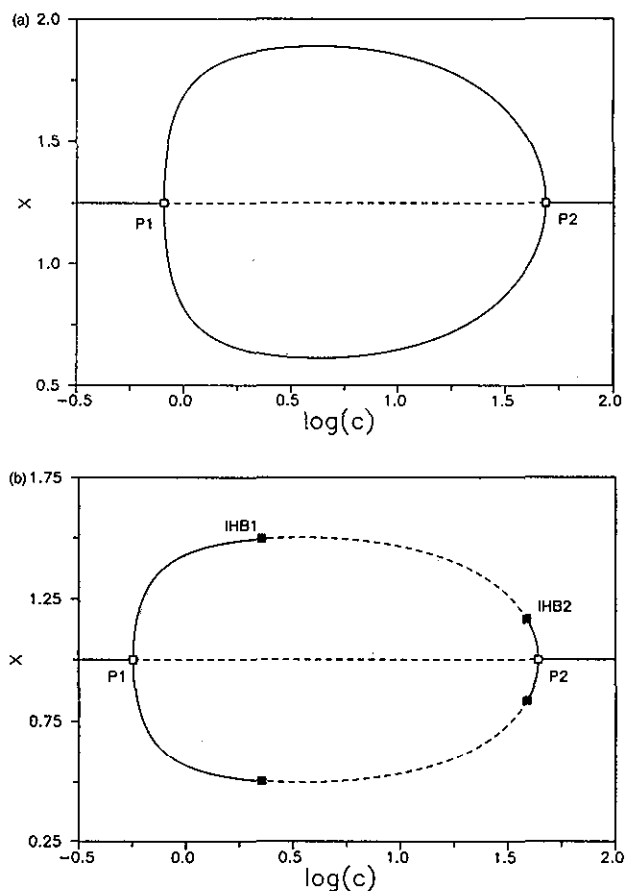FIG. 2. Bifurcation diagram for the coupled Brusselator model. Fixed parameters: (a) $(A,B,D_x,D_y) = (1.25, 2.0, 10^{-2}, 1)$, (b) $(A,B,D_x, D_y) = (1, 1.9, 10^{-2}, 1)$.
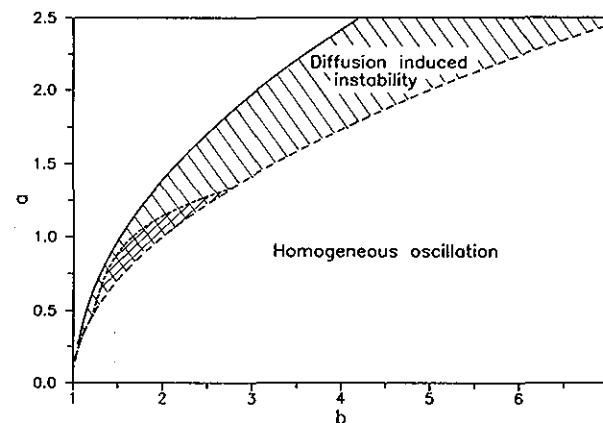

FIG. 3. Bifurcation sets in the $(b-a)$ plane for the Brusselator model (bifurcation structures generated by coupling of two oscillatory cells are not shown inside the range of homogeneous oscillation). Fixed parameters: $(D_x, D_y, c) = (10^{-2}, 1, 1)$.
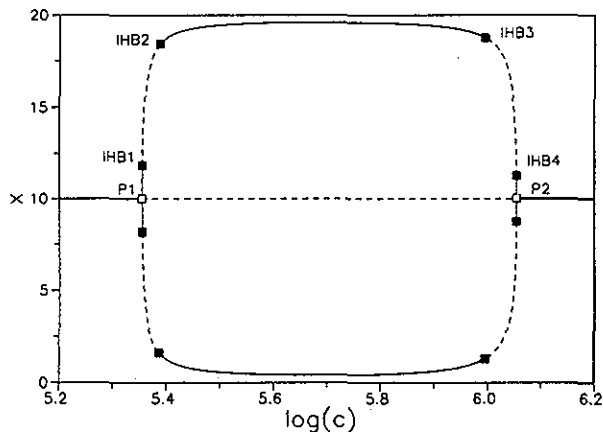
FIG. 4. Bifurcation diagram for the model, Eq. (17), of the chlorine dioxide–iodide–malonic acid reaction. Fixed parameters: $(a,b,D_x,D_y) = (50,31,10^{-6},1.5\times10^{-5})$.

FIG. 5. Bifurcation sets in the $[\log(c)\text{-}b]$ plane for the model of the chlorine dioxide–iodide–malonic acid reaction. Fixed parameters $(a,D_x,D_y) = (50,10^{-6},1.5\times10^{-5})$.

used successfully to simulate the Turing instability observed in a one-dimensional distributed system. The reactions are

$$A \rightarrow X,$$

$$X \rightarrow Y, \tag{16}$$

$$4X + Y \rightarrow P,$$

which lead to the following kinetic equations in dimensionless form:

$$\dot{x} = a - x - 4[xy/(1+x^2)],$$
$$\dot{y} = b[x - xy/(1+x^2)]. \tag{17}$$

The steady-state solution $(x_{ss} = a/5, y_{ss} = 1 + a^2/25)$ is stable if $b > (3/5)a - 25/a$.

The dynamical behavior of the coupled system is somewhat more complicated than in the case of the Brusselator. The one-parameter bifurcation diagram in Fig. 4 shows that soon after the first pitchfork bifurcation P1 the new inhomogeneous steady states lose stability through supercritical Hopf bifurcation at IHB1, but later regain stability through another supercritical Hopf bifurcation IHB2. Between the two Hopf bifurcations we have out-of-phase oscillations in the two reactors. The same bifurcation sequence is found as c is decreased through the upper pitchfork bifurcation P2. We thus have four Hopf bifurcation points on the same branch of states.

The result of following the Hopf bifurcation in two parameters with b as the secondary bifurcation parameter is shown in Fig. 5. The range of diffusion-induced instability is inside the solid lines above the horizontal dashed homogeneous Hopf bifurcation line. Three regions can be distinguished. In the regions above the upper Hopf curve and below the lower Hopf curve the inhomogeneous steady states are stable, while in the region between these bifurcation curves we have inhomogeneous out-of-phase oscillation.

The $a - b$ two-parameter bifurcation diagram, Fig. 6, differs qualitatively from the corresponding diagram for
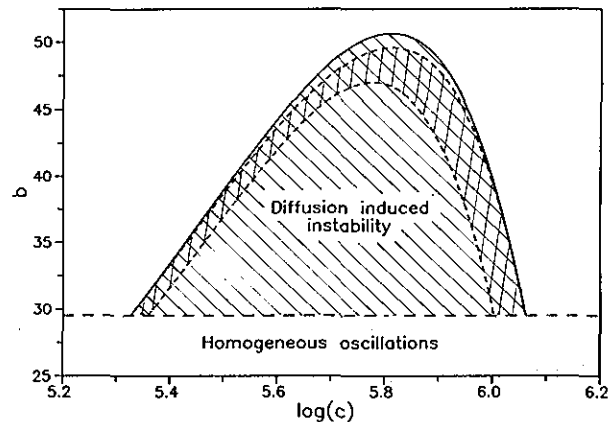
the Brusselator, Fig. 3, in that here the region of diffusion-induced oscillation is open upward, while in the Brusselator oscillatory behavior can occur only in a closed range of parameters. The range of diffusion-induced instability lies between the homogeneous Hopf bifurcation curve and the solid pitchfork bifurcation curve. A second curve of inhomogeneous Hopf bifurcations cannot be seen here, because it is so close to the pitchfork bifurcation curve as to make the two curves indistinguishable on this scale.

VI. THE DEGN–HARRISON MODEL

The respiratory behavior of a *Klebsiella Aerogenes* bacterial culture can be described with a simple model suggested by Degn and Harrison.[20] The model consists of three steps:
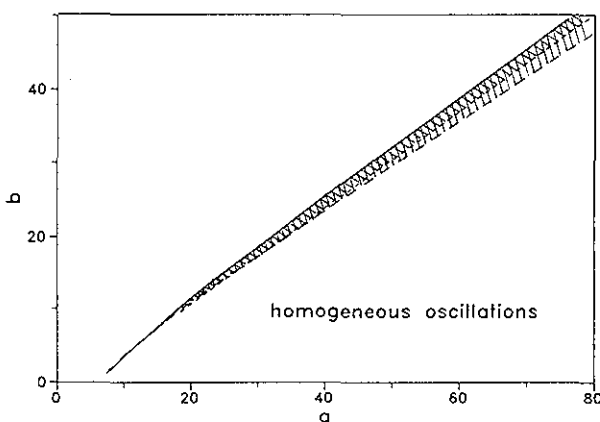
$$A \rightarrow Y,$$
$$B \rightleftharpoons X, \tag{18}$$
$$X + Y \rightarrow P,$$

FIG. 6. Bifurcation sets in the $(a - b)$ plane for the model of the chlorine dioxide–iodide–malonic acid reaction. Fixed parameters: $[D_x,D_y, \log(c)] = (10^{-6},1.5\times10^{-5},5.375)$.
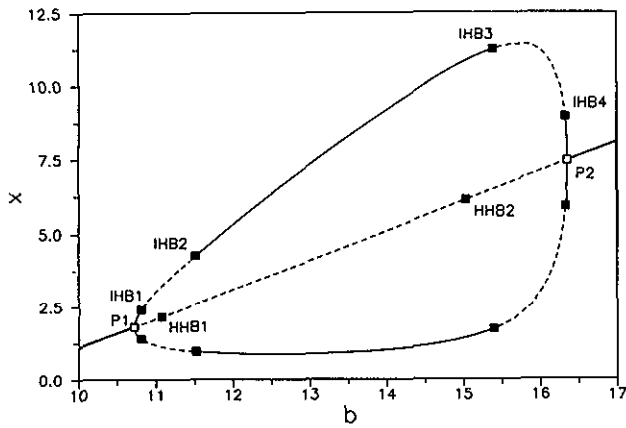
FIG. 7. Bifurcation diagram for the Degn–Harrison model. Fixed parameters: $[a,q,D_x,D_y, \log(c)] = (8.915, 0.5, 10^{-5}, 10^{-3}, 3.6)$.

FIG. 8. Bifurcation sets in the $(a-b)$ parameter plane for the Degn–Harrison model. Fixed parameters: $[q,D_x,D_y,\log(c)] = (0.5, 10^{-5}, 10^{-3}, 3.6)$.

which yield the following dimensionless equations for the temporal evolution of the system:

$$\dot{x} = b - x - xy/(1 + qx^2),$$
$$\dot{y} = a - xy/(1 + qx^2). \tag{19}$$

The model (19) has been thoroughly analyzed by Velarde et al.,[21,26] who found oscillations in a homogeneous system, and dissipative (Turing) structures and traveling waves in a continuous, inhomogeneous system. The steady-state solution of Eqs. (19) is

$$x_{ss} = b - a,$$
$$y_{ss} = a[1 - q(b-a)]/(b-a). \tag{20}$$

In contrast to the models considered above, where the steady state of the uncoupled model undergoes a single Hopf bifurcation as the parameters are changed, the uncoupled Degn–Harrison model possesses two Hopf bifurcation points, labeled HHB1 and HHB2 in the one-parameter bifurcation diagram in Fig. 7. As the parameter b is increased, the homogeneous steady state loses stability at the pitchfork bifurcation (P1) and two new inhomogeneous steady states emerge. These soon lose their stability at the inhomogeneous Hopf bifurcation (IHB1), and oscillation appears. This oscillation persists through part of the range of the homogeneous oscillation between HHB1 and HHB2, until it loses stability via the second inhomogeneous Hopf bifurcation IHB2. This scenario resembles somewhat that seen by Crowley and Epstein[27] in experiments on diffusively coupled Belousov–Zhabotinskii systems. At the right side of the diagram, the situation is slightly different, in that as b is lowered, the second inhomogeneous Hopf bifurcation occurs before we reach HHB2.

The two-parameter bifurcation diagram shown in Fig. 8 with a as the secondary bifurcation parameter is perhaps more revealing. The solid curve of pitchfork bifurcation points encloses the homogeneous Hopf bifurcation curve. There are two ranges of diffusion-induced oscillation on the upper and lower sides of the homogeneous Hopf curve.
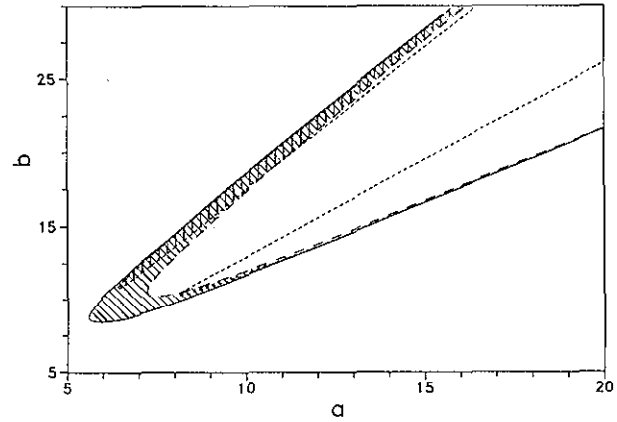
One branch of each inhomogeneous Hopf curve in Fig. 8 is situated outside the homogeneous Hopf curve while the other lies inside, suggesting the possibility of strong interaction between the various bifurcation points and raising the question of the stability of the several coexisting oscillatory modes. In Fig. 9(a) and (b) we show the amplitude
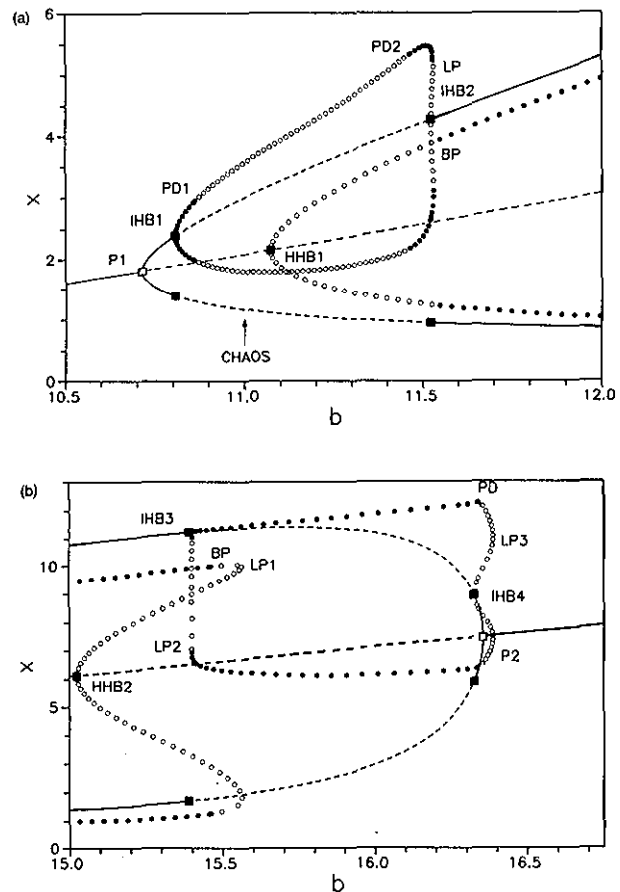

FIG. 9. Bifurcation diagrams for the Degn–Harrison model for expanded regions of Fig. 7 showing the amplitude of the oscillations.
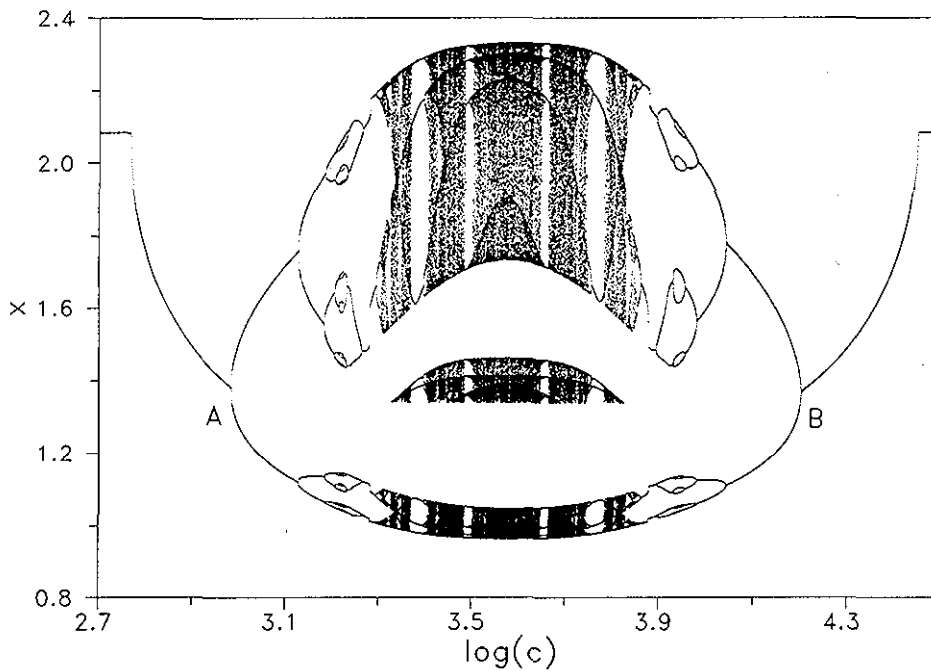
FIG. 10. Bifurcation diagram for the Degn–Harrison model. Fixed parameters: $(a,b,q,D_x,D_y) = (8.951,11.0,0.5,10^{-5},10^{-3})$.

of the oscillations in the regions around the pitchfork bifurcation points of Fig. 7. As we increase b in Fig. 9(a), before reaching HHB1 we encounter a period doubling (PD1) sequence followed by chaotic behavior. Further on, the character of the homogeneous Hopf bifurcation (HHB2) has changed from supercritical in the uncoupled system to subcritical, as a result of the interaction of the pitchfork bifurcation with the homogeneous and inhomogeneous Hopf bifurcations. The diffusion-induced homogeneous oscillation also exhibits a period doubling sequence in a narrow range of b just beyond the pitchfork bifurcation point [PD in Fig. 9(b)].

We can gain further insight into the dynamics of the coupled system by varying the coupling parameter c. We choose a value of b outside the oscillatory range of the uncoupled system and vary c. The result is shown in Fig. 10. If c lies outside a critical range, the homogeneous steady state is stable. Within the range of diffusion-induced instability, we see first the emergence of a pair of stable inhomogeneous steady states. For clarity, we show only one branch of the steady-state solution. As c is increased further, the inhomogeneous steady state becomes unstable and oscillations appear. Between points A and B in Fig. 10 we show the maximum and the minimum of the oscillations. After period doubling and inverse period doubling sequences, chaos appears in a rather wide range of c, with windows of complex periodic behavior separating several chaotic subregions. In Fig. 11 we give an indication of the effect of the diffusion coefficients. On varying D_x, we observe both simple and complex oscillatory behavior as well as hysteresis among different oscillatory modes. The complexity of the behavior of this simple model is remarkable.

VII. DISCUSSION

We have dealt here with two-variable models because they offer the prospect of obtaining at least some results analytically. The numerical integration and continuation methods that we have employed can easily be applied to more complex, many-variable models. Real experimental systems can rarely be described with such simple models, so one may expect the bifurcation diagram of the uncoupled system to be significantly more complicated than the ones treated here. Our last example shows that the interaction of two or more bifurcation points can generate very complex temporal behavior in the individual reactors, and that various combinations of homogeneous and inhomogeneous oscillations, chaos and steady states can coexist in a range of parameters where the uncoupled system has just a single stable steady state. In open systems, multiple stable steady states can exist outside the range of oscillation, and their destabilization by diffusion can lead to dynamical complexity at least as dramatic as that seen in the Degn–
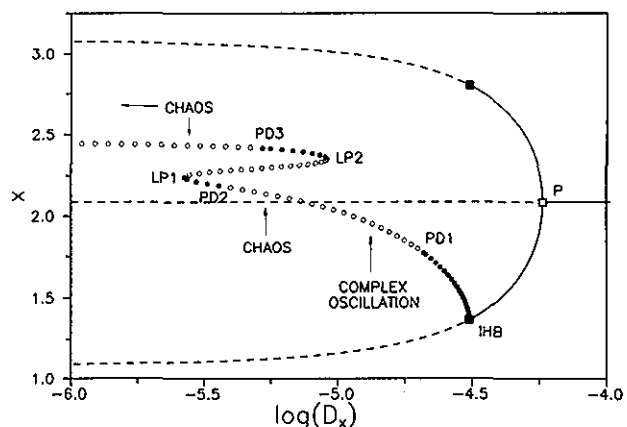

FIG. 11. Bifurcation diagram for the Degn–Harrison model. Maximum of oscillation on one solution branch is shown. Fixed parameters: $[a,b, q, \log(c),D_y] = (8.951,11.0, 0.5,3.6,10^{-3})$.

Harrison model. Consequently, it should not be surprising if real biological and chemical systems can produce exceedingly complex temporal behavior, including chaos, originating from "simple subsystems."

Diffusion-induced instability has not been investigated experimentally under the conditions treated here. Oscillatory chemical reactions may provide a useful starting point for the design of such experiments, since all models we have studied that give rise to homogeneous oscillatory behavior also show diffusion-induced instability under steady-state conditions close to the oscillatory state. It might appear that all that is needed is to choose a reaction and run it in a pair of flow reactors with identical feeds and separated by a semipermeable membrane. However, there are several important additional conditions that must be met. A key issue is the volume of the reactors. Simple calculations show that diffusion-induced instability will require a high value of c because of the small diffusion coefficients. Thus we need a reactor with a small volume and a very thin membrane with a large surface area. While it is possible to design and build reactors with a volume of, for example, 1 cm^3 and a thin plate geometry, the problem of mixing within the reactors becomes a serious one.

Another major obstacle in designing experiments is that for diffusion-induced instability the diffusion coefficient of the activator (e.g., the autocatalyst) must be smaller than that of the inhibitor by about an order of magnitude. However, for typical small inorganic molecules the diffusion coefficients are all in the same range, about 1.5×10^{-5} cm^2 s^{-1} in water at room temperature. Lengyel and Epstein[19] showed that in the chlorite–iodide–malonic acid and chlorine dioxide–iodide(iodine)–malonic acid reactions, it is possible to create the required difference between the diffusivities of iodide and chlorite ions. In the presence of starch or an appropriate organic polymer, iodine and triiodide ions are bound to the large organic molecules and lose their mobility. As iodide ions become tied up in immobile triiodide complexes, the free diffusible iodide concentration is effectively reduced by a factor of 10 or more. The experimental observation of Turing structures in the chlorite–iodide–malonic acid reaction in a gel reactor[25] was explained by this mechanism. One could similarly build a pair of coupled reactors in which the semipermeable membrane was loaded with starch to slow the diffusion of iodide.

It is not easy to find other oscillatory reactions for which a similar artifice might be employed. The bromate-based oscillators[28] offer little prospect for slowing the diffusion of the activator species HBrO$_2$ or BrO$_2$. It is even harder to imagine specific effects in the multitude of pH-driven oscillators[29] to make the activator hydrogen ion diffuse less rapidly than the various larger inhibitor species. Sulfur-based reactions or transition metal oscillators may offer better prospects for finding systems in which the autocatalytic species can form stable complexes with an immobile matrix that makes its diffusion slower.

In biological systems, the high surface/volume ratio and thin membrane walls of cells and the large differences between diffusion coefficients resulting from the wide range of molecular sizes and strengths of interactions with membranes make it far easier to realize the necessary conditions for diffusion-induced instability. Substrate inhibition and autocatalysis are common features of enzyme-regulated processes. It seems likely that nature has already discovered and made use of the dynamical possibilities of diffusion-induced instability to generate some of the wide variety of temporal behavior found in living systems.

[1] M. Marek and E. Svobodova, Biophys. Chem. **3**, 263 (1975).

[2] M. F. Crowley and R. J. Field, J. Phys. Chem. **90**, 1907 (1986).

[3] M. Alamgir and I. R. Epstein, J. Am. Chem. Soc. **105**, 2500 (1983).

[4] A. M. Turing, Philos. Trans. R. Soc. London Sect. B **237**, 37 (1952).

[5] H. Meinhardt, *Models of Biological Pattern Formation* (Academic, London, 1982).

[6] J. D. Murray, *Mathematical Biology* (Springer-Verlag, Berlin, 1989).

[7] I. Prigogine and R. Lefever, J. Chem. Phys. **48**, 1695 (1968).

[8] J. J. Tyson and S. Kauffman, J. Math. Biol. **1**, 289 (1975).

[9] I. Schreiber, M. Holodniok, M. Kubíček, and M. Marek, J. Stat. Phys. **43**, 489 (1986).

[10] P. Ortoleva and J. Ross, Biophys. Chem. **1**, 87 (1973).

[11] I. R. Epstein, J. Chem. Phys. **92**, 1702 (1990).

[12] D. Winston, M. Arora, J. Maselko, V. Gáspár, and K. Showalter, Nature **351**, 132 (1991).

[13] L. A. Segel, *Modeling Dynamic Phenomena in Molecular and Cellular Biology* (Cambridge U.P., New York, 1984).

[14] L. Edelstein-Keshet, *Mathematical Models in Biology* (Random House, New York, 1988).

[15] M. Kubíček and M. Marek, *Computational Methods in Bifurcation Theory and Dissipative Structures* (Springer-Verlag, New York, 1983).

[16] R. Seydel, *From Equilibrium to Chaos: Practical Bifurcation and Stability Analysis* (Elsevier, New York, 1988).

[17] E. J. Doedel and J. P. Kernevez, *AUTO: Software for Continuation and Bifurcation Problems in Ordinary Differential Equations*, Tech. Rep., Applied Mathematics, California Institute of Technology (1986).

[18] I. Lengyel, G. Rábai, and I. R. Epstein, J. Am. Chem. Soc. **112**, 9104 (1990).

[19] I. Lengyel and I. R. Epstein, Science **251**, 650 (1991).

[20] H. Degn and D. E. F. Harrison, J. Theor. Biol. **22**, 238 (1969).

[21] V. Fairén and M. G. Velarde, Prog. Theor. Phys. **61**, 801 (1979).

[22] G. Nicolis and I. Prigogine, *Self-Organization in Nonequilibrium Systems* (Wiley, New York, 1977).

[23] M. Boukalouch, J. Elezgaray, A. Arneodo, J. Boissonade, and P. De Kepper, J. Phys. Chem. **91**, 5843 (1987).

[24] I. Lengyel, G. Rábai, and I. R. Epstein, J. Am. Chem. Soc. **112**, 4606 (1990).

[25] V. Castets, E. Dulos, J. Boissonade, and P. De Kepper, Phys. Rev. Lett. **64**, 2953 (1990).

[26] J. L. Ibañez, V. Fairén, and M. G. Velarde, Phys. Lett. A **59**, 355 (1976).

[27] M. F. Crowley and I. R. Epstein, J. Phys. Chem. **93**, 2496 (1989).

[28] *Oscillations and Traveling Waves in Chemical Systems*, edited by R. J. Field and M. Burger (Wiley, New York, 1985), Chaps. 2–4.

[29] G. Rábai, M. Orbán, and I. R. Epstein, Acc. Chem. Res. **23**, 258 (1990).